arXiv:1212.5237v1 [quant-ph] 20 Dec 2012

Coherence-Enhanced Spaser

Konstantin E. Dorfman^{1,2,*} Pankaj K. Jha^{1,3,†} and Dmitri V. Voronine^{1,3},
Patrice Genevet^{4}, Federico Capasso^{4} and Marlan O. Scully^{1,3,5}
^{1}*Texas A&M University, College Station, Texas 77843, USA*
^{2}*University of California Irvine, California 92697, USA*
^{3}*Princeton University, Princeton, New Jersey 08544, USA*
^{4}*Harvard University, Cambridge, Massachusetts 02138, USA*
^{5}*Baylor University Waco, Texas 76798, USA*

(Dated: December 21, 2012)

We investigate surface plasmon amplification in a silver nanoshell coupled to an externally driven three-level gain medium, and show that quantum coherence significantly enhances the generation of surface plasmons. Surface plasmon amplification by stimulated emission of radiation is achieved in the absence of population inversion on the spasing transition, which reduces the pump requirements. The coherent drive allows us to control the dynamics, and holds promise for quantum control of nanoplasmonic devices.

PACS numbers: 78.67.-n,42.50.-p,78.20Bh,78.45.+h

Quantum nanoplasmonics is a promising active field of research which involves quantum mechanical control of plasmon resonances [1, 2], quantum optical applications using plasmons [3, 4] and the development of active plasmonic devices [5]. Surface plasmons (SPs) localize the light within subwavelength volumes which makes them an ideal tool for enhancing and controlling the light-matter interaction at the nanoscale. The possibility of amplifying SPs by stimulated emission thus generates highly localized and coherent optical fields in smaller volumes. It is attractive from both fundamental and application points of view [5–8]. Spasers have been experimentally demonstrated recently [9–11] and may find applications, for example, in sensing, bio-imaging and spectroscopy [12].

Several technical challenges, however, must be overcome in order to realize reliable, efficient, high-gain spasers. First, spasers have high thresholds which may limit their use in applications [13]. Second, in addition to the threshold problem, spasers have low efficiencies, generating only few plasmons per spasing mode [5–8]. These limitations of spasers with two-level gain medium are related to the effect of gain saturation caused by the feedback of SP modes on the gain medium. After a short time, absorption and emission become equal, leading to saturation. One way to circumvent this is by adding a saturable absorber (bistable spaser) [8] which poses technological challenges. Moreover, further increase of the input field intensity leads to extra Ohmic losses due to heating of the metallic surface.

The field of nanophotonics would benefit from the development of nanoscale coherent sources with increased field intensity output, lower threshold and with performance controlled via external fields. In this Letter, we apply a concept similar to lasing without inversion (LWI) [14–18] to SP generation and amplification. Three-level systems experience Fano-type interference in their absorption profile due to two possible absorption paths [15]. This Fano-type interference generates an asymmetry between absorption and stimulated emission which may lead to LWI. We consider a three-level gain medium with one of the transitions coupled to a plasmon mode. Using quantum coherence, we mitigate the SP absorption, achieving gain even without population inversion on the spasing transition in the steady-state regime. We theoretically demonstrate that the performance of an externally driven three-level spaser may be enhanced compared to conventional two-level spasers. The introduction of an external driving field that controls the quantum coherence in the gain medium decreases the spasing threshold and increases the number of SPs. We show that coherence-enhanced spasers can be robust against decoherence and that the coherent drive provides

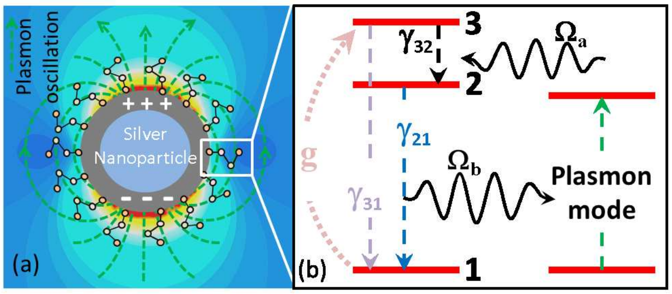

FIG. 1. Schematic of the coherence-enhanced spaser. (a) A silver nanoshell surrounded by three-level gain medium chromophores such as atoms, molecules or semiconductor quantum dots placed in the near field of a dipolar plasmon mode. (b) The three-level gain medium is excited by an external incoherent pump g to the upper state $|3\rangle$ which decays to states $|1\rangle$ and $|2\rangle$. The $|2\rangle \rightarrow |1\rangle$ transition is nearly resonant with the plasmon mode of the silver nanoshell such that the state $|2\rangle$ decays by emitting SPs via energy transfer. The plasmonic oscillations of the nanoshell stimulate this emission, supplying coherent feedback for the spaser. The physical mechanisms involved in the spasing process are analogous to electromagnetically induced transparency and coherent population trapping: an external coherent drive Ω_a is applied to the transition $|2\rangle \rightarrow |3\rangle$ creating an asymmetry between absorption and stimulated emission on the spasing transition $|2\rangle \rightarrow |1\rangle$, enabling spasing without population inversion.

a means to control their dynamics.

The spasing process in a nanosystem with a three-level gain medium is shown in Fig. 1. The gain medium is a generic system of three-level chromophores such as atoms, molecules or semiconductor quantum dots, which have a ground state $|1\rangle$ and two excited states $|2\rangle$ and $|3\rangle$. An incoherent pumping source couples states $|1\rangle$ and $|3\rangle$. Transition $|2\rangle \rightarrow |3\rangle$ is driven by an external coherent source as in the standard LWI theory [15]. Transition $|2\rangle \rightarrow |1\rangle$ which occurs spontaneously is nearly resonant to the plasmon mode of a metallic nanostructure such as a silver nanoshell and is used to transfer energy from the gain medium to SPs. The local field of SPs in turn provides feedback by stimulating the $|2\rangle \rightarrow |1\rangle$ transition.

The SP eigenmodes $\phi_n(\mathbf{r})$ are described by a wave equation $\nabla[\Theta(\mathbf{r})\nabla\phi_n(\mathbf{r})] = s_n\nabla^2\phi_n(\mathbf{r})$, where s_n is a real eigenvalue ($0 \leq s_n \leq 1$) corresponding to a plasmon mode n [19]. The characteristic function $\Theta(\mathbf{r})$ is equal to 1 for the metal and 0 for the dielectric. The SP frequency ω_n is defined by $Re[s(\omega_n)] = s_n$, where $s(\omega) = \epsilon_d/[\epsilon_d - \epsilon_m(\omega)]$ is the spectral parameter, ϵ_d is the dielectric permittivity, and $\epsilon_m(\omega)$ is the permittivity of the metal. The spaser Hamiltonian is $\mathscr{H} = \mathscr{H}_{pl} + \mathscr{H}_{ph} + \mathscr{H}_{int}$, where the plasmon and photon Hamiltonians are given by $\mathscr{H}_{pl} = \hbar\sum_n \omega_n \hat{a}_n^\dagger \hat{a}_n$, $\mathscr{H}_{ph} = \hbar\sum_m \omega_m \hat{b}_m^\dagger \hat{b}_m$, while the interaction Hamiltonian is $\mathscr{H}_{int} = -\sum_p \mathbf{E}(\mathbf{r}_p)\mathbf{d}^{(p)}$, that includes the plasmon-chromophore $|2\rangle \rightarrow |1\rangle$ and photon-chromophore $|2\rangle \rightarrow |3\rangle$ interactions. Here p is an index of the pth gain medium chromophore (atom, molecule or quantum dot) with a position $\mathbf{r}_p$ and a transition dipole moment $\mathbf{d}^{(p)}$, $\hat{a}_n$ and $\hat{a}_n^\dagger$ are annihilation and creation operators of the n^{th} plasmon, $\hat{b}_m$ and $\hat{b}_m^\dagger$ are annihilation and creation operators of the m^{th} photon, respectively. The electric field consists of two parts, $\mathbf{E}(\mathbf{r}) = \mathbf{E}_{pl}(\mathbf{r}) + \mathbf{E}_{ext}(\mathbf{r})$. The electric field of the quantized surface plasmons is $\mathbf{E}_{pl}(\mathbf{r}) = -\sum_n A_n\nabla\phi_n(\mathbf{r})(\hat{a}_n^\dagger + \hat{a}_n)$, $A_n = \left(\frac{4\pi\hbar s_n}{\epsilon_d s_n'}\right)^{1/2}$, where $s_n' = Re[ds(\omega_n)/d\omega_n]$ and the electric field of the external photon drive is $\mathbf{E}_{ext}(\mathbf{r}) = -\sum_m \mathbf{E}_m(\mathbf{r})(\hat{b}_m^\dagger + \hat{b}_m)$, where $\mathbf{E}_m(\mathbf{r})$ is an amplitude of the m-th mode.

In this work, as in standard semi-classical laser theory, we treat the gain medium quantum mechanically, and the SPs and photons classically. We consider the operators $\hat{a}_n$ and $\hat{b}_m$ as complex numbers a_n and b_m, respectively, with the time dependence $a_n = a_{0n}e^{-i\nu_s t}$ and $b_m = b_{0m}e^{-i\nu_{23}t}$, where a_{0n} and b_{0m} are slowly varying amplitudes. Therefore, the number of coherent SPs per spasing mode is given by $N_n = |a_{0n}|^2$. Note, that in this model we assume that, unlike the transition $|2\rangle \rightarrow |1\rangle$ which is nearly resonant with the plasmons, the transition $|3\rangle \rightarrow |2\rangle$ driven by a photon source is not coupled to the metallic nanostructure and does not excite SPs. The coherence on the transition $|2\rangle \rightarrow |3\rangle$ is maintained by an external source Ω_a (Fig. 1).

It is more convenient to rewrite the interaction term, in braket notation, with rotating wave approximation as

$$\mathscr{H}_{int} = -\hbar\sum_p \left(\Omega_b^{(p)} e^{i\Delta_b t}|2\rangle\langle 1| + \Omega_a^{(p)} e^{i\Delta_a t}|3\rangle\langle 2| + \text{c.c}\right), \tag{1}$$

where $\Omega_b^{(p)} = -A_n\mathbf{d}_{21}^{(p)}\nabla\phi_n(\mathbf{r}_p)a_{0n}/\hbar$ is the Rabi frequency for the spasing transition $|2\rangle \rightarrow |1\rangle$, $\Omega_a^{(p)} = -\mathbf{E}_m(\mathbf{r}_p)\mathbf{d}_{23}^{(p)}b_{0m}/\hbar$ is the Rabi frequency for the driving transition $|2\rangle \rightarrow |3\rangle$. We define detunings as $\Delta_b = \omega_{21} - \nu_b$ and $\Delta_a = \omega_{32} - \nu_a$. Furthermore we assume that the driving field is strong enough so that the number of photons in the mode m is fixed and does not change with time. Thus, $\Omega_a^{(p)}$ is a constant, i.e. independent of time.

Introducing $\rho^{(p)}$ as a density matrix of the pth gain-medium chromophore, we derive the time evolution equations by using the Schrödinger equation

$$i\hbar\dot{\rho}^{(p)} = [\mathscr{H}, \rho^{(p)}] \tag{2}$$

as discussed in [15]. Eq. 2 includes the relaxation rates $\Gamma_{21} = \frac{1}{2}(\gamma_{21} + g) + \gamma_{ph,12} + i\Delta_b$, $\Gamma_{31} = \frac{1}{2}(\gamma_{31} + \gamma_{32} + g) + \gamma_{ph,31} + i(\Delta_a + \Delta_b)$, and $\Gamma_{32} = \frac{1}{2}(\gamma_{31} + \gamma_{21} + \gamma_{32}) + \gamma_{ph,32} + i\Delta_a$ where γ_{ij} are the spontaneous decay rates for populations, γ_{ph} are the associated dephasing rates which, for simplicity, are assumed to be equal, and g is the incoherent pump rate.

The SP stimulated emission is described as excitation by the coherent polarization of the gain medium corresponding to the transition $|2\rangle \rightarrow |1\rangle$. The corresponding time evolution equation is obtained using the Heisenberg equation of motion for a_{0_n} and adding the SP relaxation rate γ_n. It has a similar form to the equation for the two-level gain medium [8]:

$$\dot{a}_{0_n} = -\Gamma_n a_{0_n} + i\sum_p \varrho_{21}^{(p)}\tilde{\Omega}_b^{(p)}, \tag{3}$$

where $\Gamma_n = \gamma_n + i\Delta_n$, $\tilde{\Omega}_b^{(p)} = -A_n\mathbf{d}_{21}^{(p)}\nabla\phi_n(\mathbf{r}_p)/\hbar = \Omega_b^{(p)}/a_{0_n}$ is a single plasmon Rabi frequency. We assume that the Rabi frequencies are the same for all chromophores and omit the index (p) below.

To determine the spasing condition, we assume resonant coupling on the driving transition (i.e. $\Delta_a = 0$), real fields and $\Omega_b \ll \Omega_a, \Gamma_{21}$. In this limit we keep all the terms for the driving field Ω_a and restrict the field Ω_b to the lowest order. The steady-state population inversions are $\bar{n}_{21} = [(g\gamma_{32} - \gamma_{21}\gamma_{31} - \gamma_{21}\gamma_{32})\Gamma_{32} + 2(g - \gamma_{21} - \gamma_{31})\Omega_a^2]\mathcal{M}$ and $\bar{n}_{32} = (\gamma_{21} - \gamma_{32})g\Gamma_{32}\mathcal{M}$, where $\mathcal{M}^{-1} = \Gamma_{32}[g(\gamma_{21} + \gamma_{32}) + \gamma_{21}(\gamma_{31} + \gamma_{32})] + 2(2g + \gamma_{21} + \gamma_{31})\Omega_a^2$. This yields the necessary condition for the existence of a steady-state solution

$$\frac{N_p\tilde{\Omega}_b^2}{\Gamma_n\Gamma_{21}}\left(\bar{n}_{21} + \frac{\Omega_a^2}{\Gamma_{31}\Gamma_{32}}\bar{n}_{32}\right) - \frac{\Omega_a^2}{\Gamma_{21}\Gamma_{31}} = 1, \tag{4}$$

where N_p is the number of gain-medium chromophores. The condition in Eq.(4) which is valid both below and above the spaser threshold, explicitly includes the coherent drive Ω_a, thus allowing control not only of the spasing threshold but also the spasing frequency and dynamics. In the absence of the drive ($\Omega_a = 0$) and for the fast $|3\rangle \rightarrow |2\rangle$ population transfer ($\gamma_{32} \gg g$) Eq.(4) reduces to the spasing condition for a two-level system [8] as $(\nu_s - \omega_n + i\gamma_n)^{-1}(\nu_s - \omega_{21} + i\tilde{\Gamma}_{21})^{-1} N_p \tilde{\Omega}_b^2 \bar{n}_{21} = -1$, where $\tilde{\Gamma}_{ji}$=Re[Γ_{ji}]. The spasing frequency can be found from Eq. (4):

$$\nu_s = \frac{\alpha\omega_{21} + \left(\tilde{\Gamma}_{21}\tilde{\Gamma}_{31} + \Omega_a^2\right)\omega_n}{\alpha + \left(\tilde{\Gamma}_{21}\tilde{\Gamma}_{31} + \Omega_a^2\right)}, \tag{5}$$

where $\alpha = \left[\left(N_p \tilde{\Omega}_b^2/\Gamma_{32}\tilde{\Gamma}_{31}\right)\bar{n}_{32} - \gamma_n/\tilde{\Gamma}_{31}\right]\Omega_a^2 + \gamma_n\tilde{\Gamma}_{31}$. In the absence of the driving field, Eq.(5) reduces to $\nu_s = (\gamma_n\omega_{21} + \tilde{\Gamma}_{21}\omega_n)/(\gamma_n + \tilde{\Gamma}_{21})$ which is identical to Eq.(11) of ref. [8]. Also, in the absence of the driving field, the spasing frequency is given by a combination of the atomic and the plasmonic resonances. Eq.(5) shows that the driving field modifies the spasing frequency, providing a new external control parameter.

Within a certain range of parameters, it is possible to study the problem analytically. In particular, if $\gamma_{31} \ll \gamma_{32} \ll \gamma_{21}$, in the limit of a strong drive, $\Omega_a \gg \gamma_{21}, \gamma_n$, in the vicinity of the threshold $g \sim \gamma_{12}$, the number of surface plasmons is independent of the driving field and is given for $g > \gamma_{21}$ by $N_n \simeq \frac{N_p}{6\gamma_n}(g - \gamma_{21})$. On the other hand, if the driving is weak, $\Omega_a \ll \gamma_{12}, \gamma_n$, then a similar analysis yields $N_n \simeq \frac{N_p}{2\gamma_n}\frac{\gamma_{32}}{\gamma_{21}}(g - \gamma_{21})$. In the weak drive limit, the linear increment of N_n is smaller, because $\gamma_{32} \ll \gamma_{21}$. Therefore, coherent driving can substantially enhance the number of stimulated surface plasmons.

Next we present the numerical simulation results obtained by solving the system of equations Eq.(2). We consider the lower transition $|2\rangle \leftrightarrow |1\rangle$ of the three-level gain medium coupled to a dipolar SP mode of a silver nanoshell with $\hbar\omega_n = 2.5$ eV. The detuning of the gain medium from the SP mode is $\hbar(\omega_{21} - \omega_n)$ = 0.002 eV. The core of the nanoshell and the external dielectric have the same permittivity of ϵ_d = 2.25. The permittivity of silver was taken from ref. [22]. The gain medium is modeled using the following spontaneous decay rates: γ_{21} = 4×10^{12} s^{-1}, γ_{31} = 4×10^{10} s^{-1}, and γ_{32} = 4×10^{11} s^{-1}; the detunings Δ_a and Δ_b are set to zero. Note that the value of γ_{21} is identical to the one in Ref. [6] and that the other rates were chosen according to the criteria for LWI [16, 17]. The nanoshell SP damping rate is γ_n = 5.3×10^{14} s^{-1} with Δ_n = 3×10^{12} s^{-1}. The number of gain medium chromophores is $N_p \simeq 6 \times 10^4$. The latter has been chosen to match the density of chromophores in [6].

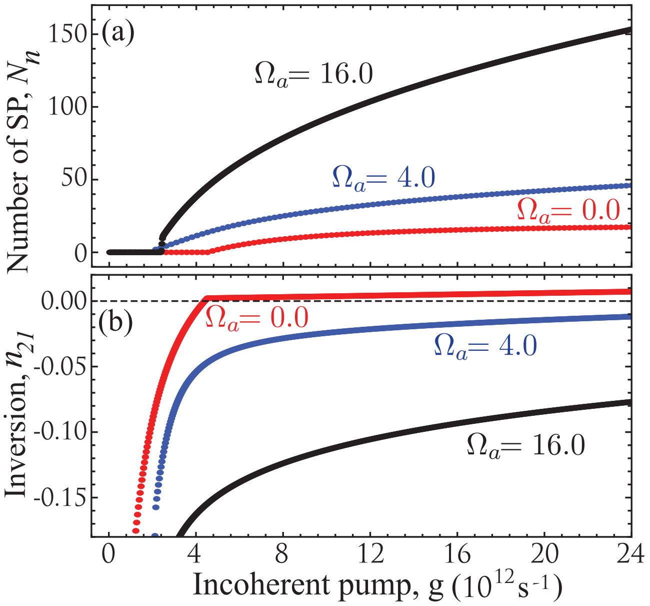

FIG. 2. Steady-state properties of a three-level silver nanoshell spaser with $\hbar\omega_n$ = 2.5 eV as a function of the incoherent pumping rate g for three driving fields: Ω_a = 0 (red), 4×10^{12} s^{-1} (blue) and 16×10^{12} s^{-1} (black). The dephasing rate γ_{ph} = 0 . Note that the effect of decoherence are studied in a separate plot in Fig.3. (a) Number N_n of plasmons per spasing mode. Interestingly, Ω_a not only controls the spaser threshold but it also controls the number of generated plasmons. (b) Population inversion (n_{21}) on the spasing transition $|2\rangle \leftrightarrow |1\rangle$. Coherent drive allows obtaining a large enhancement of a number of plasmons in the absence of population inversion at the spasing frequency and reduces the spasing threshold.

Fig. 2(a), obtained by solving the system Eq 2 for different values of Rabi frequency Ω_a, shows the number of SPs N_n generated in the presence of the coherent drive Ω_a for the dephasing rate γ_{ph} = 0. N_n is enhanced by an order of magnitude for higher values of the pumping rate g. This is accompanied by a factor of two decrease of the spasing threshold. Fig. 2(b) shows population inversion on the spasing transition $|2\rangle \leftrightarrow |1\rangle$ for the three choices of drive Rabi frequency Ω_a considered in Fig 2(a). The enhancement of the number of plasmons corresponds to a decrease of the population inversion on the spasing transition. At the same time the overall excited states population inversion ($\rho_{22} + \rho_{33} - \rho_{11}$) is positive. The enhancement is due to the quantum coherence in the three-level gain medium generated by the drive Ω_a, i. e. breaking of detailed balance on the spasing transition. It is worth noticing two things: first, the coherent drive is applied at a different frequency than both the incoherent pumping or the spasing frequencies; being not resonant with the plasmon mode, we can achieve strong driving field without damaging the nanoparticles. Second, the control of the output can be achieved at low plasmon numbers which may be useful for single plasmon engineering [4] and applications in quantum nanophotonics.

To reveal the role of decoherence, we show the number of SPs N_n versus the incoherent pumping rate g for different dephasing rates $\gamma_{ph} = 0, 80, 160$, and 240×10^{12} s^{-1} in Fig. 3. Even in the case of a large dephasing rate $\gamma_{ph} = 80 \times 10^{12}$ s^{-1}, which is typical for semiconductor systems, we still observe the effect of enhanced generation of SPs due to the presence of the coherent drive. Similar effects in atomic systems in the XUV and the optical domains have recently been studied [20, 21].

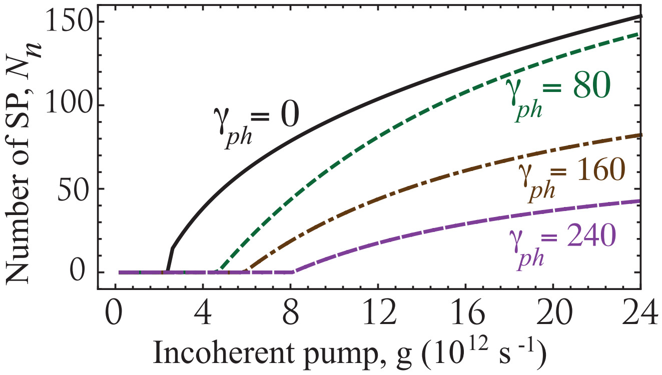

FIG. 3. Number of SPs N_n versus the incoherent pumping rate g for different dephasing rates $\gamma_{ph} = 0, 80, 160$, and $240{\times}10^{12}$ s^{-1} for Ω_a = $16{\times}10^{12}$ s^{-1}. Steady-state coherence-enhanced spasing is robust against decoherence and may be observed even for large dephasing rates.

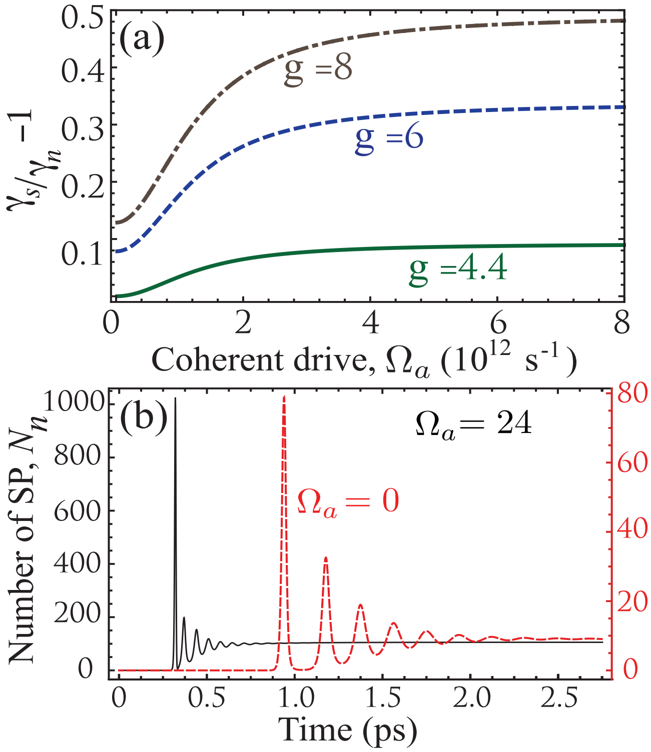

FIG. 4. (a) Ratio of the imaginary part of the Floquet exponent γ_s normalized by the SP linewidth γ_n for three values of the pumping rate g = 4.4, 6 and $8{\times}10^{12}$ s^{-1} for γ_{ph} = 0. γ_s corresponds to the growth rate of the plasmonic field and may be increased by the coherent drive. (b) Temporal profiles of the plasmonic field intensity for Ω_a = 0 and $24{\times}10^{12}$ s^{-1} show that the steady state is achieved much faster for a stronger drive. This corresponds to a larger value of γ_s which can be controlled by the drive as shown in (a).

Next we demonstrate how the spaser dynamics may be controlled by the coherent driving field. Fig. 4a shows the ratio of the imaginary part of the Floquet exponent γ_s normalized by the SP linewidth γ_n for three values of the pumping rate g = 4.4, 6 and $8{\times}10^{12}$ s^{-1} for the dephasing rate γ_{ph} = 0. Larger values of γ_s are obtained for larger values of the pump g and moderate values of the drive Ω_a. Different values of the Floquet exponent correspond to different dynamics and have been used to classify lasers [23]. Fig. 4b shows two temporal profiles of the plasmonic field intensity for Ω_a = 0 and $24{\times}10^{12}$ s^{-1} for g = $8{\times}10^{12}$ s^{-1}. Stronger drive causes the earlier onset of spasing and the faster approach to the steady state. This corresponds to a larger value of γ_s which can be controlled by the drive as shown in Fig. 4a. Such control of the spaser dynamics may be important for ultrafast nanophotonics applications.

Coherence-enhanced spaser operation can be experimentally realized by following two different approaches. The first one consists of coating plasmonic nanoparticles or clusters of nanoparticles with self-assembled layers of molecules or quantum dots. Gain and even spasing in such plasmonic nanostructures have previously been reported using a combination of two-level molecules and nanoparticles [9]. Spasing threshold values reported in various experiments confirm that this approach is unpractical for potential applications, in particular due to the large pumping energy required to achieve population inversion [13]. Using surface chemistry one can synthesize three-level molecular systems deposited on nanoparticles by e.g. self-assembly.

The second approach uses very low loss long range propagating surface plasmon polaritons (LRSPPs). These LRSPPs have been successfully amplified by depositing a doped polymer [11] or a dye-doped dielectric on top of the plasmon waveguides [24]. This scheme, where LRSPPs are amplified with surprisingly low noise due to limited mode partition noise[25], can be extended to the three-level gain medium by patterning LRSPP waveguides at the interface between three-level quantum wells.

In summary, we have proposed a new scheme for creating an efficient coherent source of radiation at the subwavelength scale. We showed that the emission properties of spasers may be enhanced using quantum coherence in a three-level gain medium placed in the near field of a plasmonic nanostructure. We demonstrated a significant spasing enhancement and reduction of the spasing threshold for moderate driving fields. We have also investigated the effect of dephasing and showed that the enhancement is robust under realistic conditions. The driving field acts as an external control parameter to tune the emission properties of the spaser such as threshold, number of generated plasmons and emission frequency. The driving field may be chosen to interact with the gain medium at a different frequency from that of the spasing transition, avoiding spurious heating effects which could degrade the performance of the device. Coherent control is achieved in a wide range of plasmon output power and persists down to the single plasmon level at low driving field intensity. Because the driving field also controls the spaser dynamics, it may lead to future ultrafast and controllable nanoplasmonic devices. These concepts may be extended to a broader range of quantum optical phenomena and applied to a variety of plasmonic nanostructures. Plasmonic structures of various sizes and shapes can be synthesized to resonantly enhance the applied coherent drive [26]. Plasmonic analogs of quantum optical effects such as plasmonic EIT [27, 28] and Fano resonances [29] may further improve controllability of spaser properties.

We gratefully acknowledge support by the National Science Foundation Grants PHY-1241032 (INSPIRECREATIV) and EEC-0540832 (MIRTHE ERC), and the Robert A. Welch Foundation (A-1261). P. K. Jha is supported by the Herman F. Heep and Minnie Belle Heep Texas A&M University Endowed Fund held and administered by the Texas A&M Foundation

---

[*] kdorfman@uci.edu

[†] Present Address: NSF Nanoscale Science and Engineering Center(NSEC), 5130 Etcheverry Hall, University of California, Berkeley, California 94720

[1] J. A. Scholl, A. L. Koh, and J. A. Dionne, Nature 483, 421 (2012).

[2] R. Esteban, A. G. Borisov, P. Nordlander, and J. Aizpurua, Nature Communications 3, 825 (2012).

[3] D. E. Chang, A. S. Sorensen, P. R. Hemmer, and M. D. Lukin, Phys. Rev. Lett. 97, 053002 (2006).

[4] R. Kolesov, B. Grotz, G. Balasubramanian, R. J. Stoehr, A. A. L. Nicolet, P. R. Hemmer, F. Jelezko, and J. Wrachtrup, Nature Physics 5, 470 (2009).

[5] M. I. Stockman, Opt. Express 19, 22029 (2011).

[6] D. J. Bergman, and M. I. Stockman, Phys. Rev. Lett. 90, 027402 (2003).

[7] M. I. Stockman, Nature Photonics 2, 327 (2008).

[8] M. I. Stockman, J. Opt. 12, 024004 (2010).

[9] M. A. Noginov, G. Zhu, A. M. Belgrave, R. Bakker, V. M. Shalaev, E. E. Narimanov, S. Stout, E. Herz, T. Suteewong, and U. Wiesner, Nature 460, 1110 (2009).

[10] R. F. Oulton, V. J. Sorger, T. Zentgraf, R.-M. Ma, C. Gladden, L. Dai, G. Bartal, and X. Zhang, Nature 461, 629 (2009).

[11] I. De Leon, P. Berini, Nature Photonics 4, 382 (2010).

[12] L. Novotny and B. Hecht *Principles of Nano-Optics*, (Cambridge University Press, 2006).

[13] J. B. Khurgin, and G. Sun, Nanophotonics. 1, 3 (2012).

[14] S. E. Harris Phys. Today 50, 36 (1997).

[15] M.O. Scully and M. S. Zubairy *Quantum Optics*, (Cambridge Press, London 1997).

[16] O. Kocharovskaya, Phys. Rep. 219, 175 (1992).

[17] M.O. Scully, S.Y. Zhu, and A. Gavrielides, Phys. Rev. Lett. 62, 2813 (1989).

[18] S. E. Harris, Phys. Rev. Lett. 62, 1033 (1989).

[19] M. I. Stockman, S. V. Faleev, and D. J. Bergman, Phys. Rev. Lett. 87, 167401 (2001).

[20] P. K. Jha, A. A. Svidzinsky and M. O. Scully, Laser Phys. Lett. 9, 368(2012).

[21] P. K. Jha, Ph.D. Dissertation, Texas A&M University, College Station, (2012).

[22] P. B. Johnson, and R. W. Christy, Phys. Rev. B 6, 4370 (1972).

[23] S. Wieczorek, B. Krauskopf, T. B. Simpson, and D. Lenstra, Phys. Rep. 416, 1 (2005).

[24] M. C. Gather, K. Meerholz, N. Danz, and K. Leosson, Nature Photonics 4, 457 (2010).

[25] I. De Leon, and P. Berini, Phys. Rev. B 83, 081414 (2011).

[26] H. Wang, D. Brandl, P. Nordlander, and N. Halas, Acc. Chem. Res. 40, 53 (2007).

[27] S. Zhang, D. Genov, Y. Wang, M. Liu, and X. Zhang, Phys. Rev. Lett. 101, 047401 (2008).

[28] N. Liu, L. Langguth, T. Weiss, J. Kastel, M. Fleischhauer, T. Pfau, and H. Giessen, Nature Materials, 8, 758 (2009).

[29] N. Verellen, Y. Sonnefraud, H. Sobhani, F. Hao, V. Moshchalkov, P. Dorpe, P. Norlander, and S. Maier, Nano Lett., 9, 1663 (2009)